Materials Research. 2025; 28(suppl. 1): e20250006
DOI: https://doi.org/10.1590/1980-5373-MR-2025-0006

Smart Polymer Blends of Poly(*N*-vinylcaprolactam) and Poly(lactic Acid)

***Grazielle R. Cerqueira*[a*], *Alysson N. G. Galvão*[b], *Djalma A. Oliveira*[a], *Rhodivam L. M. Feitosa*[a], *Yêda M. B. Almeida*[a,b], *Carolina L. Morelli*[a,c]**

[a]*Universidade Federal de Pernambuco (UFPE), Programa de Pós-Graduação em Ciência dos Materiais (PGMTR), 50670-901, Recife, PE, Brasil.*
[b]*Universidade Federal de Pernambuco (UFPE), Departamento de Engenharia Química, 50670- 901, Recife, PE, Brasil.*
[c]*Universidade Federal de Pernambuco (UFPE), Departamento de Engenharia Mecânica, 50670- 901, Recife, PE, Brasil.*

Received: January 03, 2025; Revised: June 03, 2025; Accepted: June 08, 2025

Poly(N-vinylcaprolactam) (PNVCL) is a biocompatible and thermoresponsive polymer, which presents changes in solubility at temperatures close to the physiological temperature, making it a promising biomaterial. However, its application is limited due to difficult processability in the molten state and brittleness in the solid state. To overcome these characteristics, the present work developed polymeric blends of PNVCL and poly(lactic acid) (PLA), which is a biodegradable and biocompatible polymer, varying mass concentrations of PNVCL by 40, 50 and 60%. Scanning electron microscopy (SEM) showed the formation of a heterogeneous morphology, with spherical domains dispersed in a matrix phase. Nevertheless, Fourier Transform Infrared Spectromicroscopy (micro-FTIR) analysis indicated the presence of both polymers in both phases, with a predominance of PNVCL in the dispersed phase and PLA in the matrix phase. All mixtures produced were thermoresponsive and exhibited a reversible change in optical properties with temperature, going from transparent to opaque upon heating.

Keywords: *Thermoresponsive polymers, Poly(N-vinylcaprolactam), Polymers blends, Poly(acid lactic), PNVCL/PLA blends.*

1. Introduction

Thermoresponsive polymers consist of macromolecules that exhibit a volumetric phase transition associated with changes in solubility in response to temperature variation[1,2]. Poly(*N*-vinylcaprolactam) (PNVCL) is a thermoresponsive, non-toxic and hydrolytically stable polymer that exhibits a lower critical solubility temperature (LCST) behavior at temperatures close to the physiological one[1,3-6]. It means that upon heating an aqueous PNVCL solution it can be induced the PNVCL precipitation, clouding the solution, at a temperature that can be called the phase separation temperature (T_{PS})[7,8]. This happens because, at T_{PS}, the PNVCL molecules undergo a coil to globule conformational transition becoming insoluble in water[1]. Several factors can influence the T_{PS} of PNVCL, such as molar mass, solution concentration, physical mixtures with other polymers and chemical modifications (copolymers or functionalization)[1,3,9].

Due to its thermoresponsive behavior, PNVCL has been considered in some biomedical applications, such as controlled drug release systems[10-13], tissue engineering[14-16] and smart dressings[7].

Nonetheless, PNVCL applications are limited by its difficult processability in the molten state and its high fragility in the solid state[7]. These aspects can be overcome by combining PNVCLwith other polymers, through the development of blends and copolymers, for example.

Polymer blends refer to the physical mixture of two or more polymers/copolymers in order to obtain additional properties not found in the individual materials[17-19]. Polymer blends can be of different types, based on the nature of the constituents, processing method, miscibility and morphology[19].

There are few studies related to the mixture of PNVCL with other polymers and none of them studied PLA. After a thorough search in the Scopus and Web of Science databases and a critical analysis of each one of the articles found, only 14 scientific articles were found on the subject (statistical data analyzed up to May 30, 2025). Most of the papers were related to the study of homopolymer PNVCL blends with other polymers, such as: sodium alginate[20,21], silk fibroin[22], poly(3-hexylthiophene)[23], poly(ε-caprolactone)[24], ethyl cellulose[25], poly(ethylene glycol)[26,27] and poly(pyridinium triflate)[28]. In addition, our research group has also developed thermoresponsive blends of PNVCL with thermoplastic polyurethane[7]. Articles were also found corresponding to blends of PNVCL copolymers with other homopolymers or copolymers, such as: polysulfone[29], copovidone[30,31] and chitosan[32].

Poly(lactic acid) (PLA) is a biopolymer widely used commercially, even in additive manufacturing, mainly due to its good processability, good mechanical properties, as well as being a biodegradable and biocompatible polymer,

*e-mail: grazielle.rozendo@ufpe.br
Associate Editor: Leonardo Gondim de Andrade e Silva.
Editor-in-Chief: Luiz Antonio Pessan.

favoring its application in the field of biomedicine and biotechnology, for example[33-35].

Considering these characteristics, the choice of PLA is also justified by its lower brittleness compared to PNVCL. While PNVCL has a glass transition temperature (T_g) of approximately 190°C[7], the Tg of PLA is around 60°C[36]. Thus, although PLA is classified as a rigid polymer compared to commodity polymers, the combination of PLA and PNVCL results in a promising material, as presented in this study.

2. Experimental

2.1. Materials

The monomer *N*-vinylcaprolactam (NVCL, Mw of 139.19 g.mol^{-1}, 98.0%), was acquired from Sigma-Aldrich (Brazil). Hexane (Mw of 86.18 g.mol^{-1}, 98.5%) was purchased from Dinâmica Química (Brazil), for purification of NVCL by recrystallization. For the synthesis of PNVCL, it was used the initiator 2,2'-azobis(2-methylpropionitrile) (AIBN), in 0.2M toluene solution (Mw of 164.21 g.mol^{-1}, 98.0%), obtained from Sigma-Aldrich (Brazil), and the solvent dimethyl sulfoxide (DMSO) P.A. (Mw of 78.13 g.mol^{-1}, 99.9%), from Dinâmica Química (Brazil). The poly(lactic acid) (PLA) used was acquired from the 3D printing filament from 3DFila (Brazil). The material is natural and transparent, as reported by the supplier. For preparing blends, it was used the solvent chloroform (P.A.), stabilized with amylene (Mw of 119.38 g.mol^{-1}, 99.8%), from Neon (Brazil).

2.2. PNVCL synthesis

PNVCL was synthesized by free radical polymerization. For this, a solution of the purified NVCL monomer (15% w.v^{-1}) in DMSO was obtained under magnetic stirring at room temperature. Then 0.2% of AIBN was added, related to NVCL mass, and the system was purged with argon. The reaction took place for 4 hours at 70 ºC, under magnetic stirring. After the reaction, the polymer formed was purified through three cycles of precipitation in heated distilled water (50 ºC) and solubilization in ice water (15 ºC). At the end of the washing cycles, the polymer solution in distilled water was poured onto a polytetrafluoroethylene (PTFE) plate and dried at room temperature[7].

2.3. Pure PNVCL and PLA films production

The preparation of PNVCL and PLA films consisted of solubilizing each polymer in chloroform at a solid concentration of 5% w.v^{-1}, under continuous stirring at room temperature, for 2 hours. After homogenization, the solutions were poured onto 5 cm diameter PTFE plates and dried under ambient conditions to obtain films with a thickness of around 200 µm.

Table 1. Composition and sample codes of PNVCL/PLA blend films.

Sample code	Composition (w %)	
	PNVCL	PLA
PLA	0	100
PNVCL/PLA 40/60	40	60
PNVCL/PLA 50/50	50	50
PNVCL/PLA 60/40	60	40
PNVCL	100	0

2.4. Production of PNVCL/PLA blends films

The polymer blends were prepared by varying the proportions between the pure materials, as described in Table 1, while maintaining a concentration of 5% w.v^{-1} solids in chloroform. For all blends, PNVCL and PLA solutions in chloroform were first prepared separately, under continuous stirring at room temperature, for 2 hours. After this time, the polymer solutions were mixed and stirred again for another 2 hours until complete homogenization. Finally, the solutions were transferred to 5 cm diameter PTFE plates and dried at room temperature. Blend films with a thickness of approximately 200 µm were obtained.

The selection of specific proportions of PNVCL/PLA blend aimed the systematic investigation of the influence of composition on the blend's thermoresponsiveness and its general properties. Starting from the equimolar ratio (PNVCL/PLA 50/50), formulations with higher (60/40) and lower (40/60) PNVCL content were also analyzed.

2.5. Attenuated total reflectance Fourier transform infrared spectroscopy (FTIR-ATR)

FTIR-ATR was performed using a Spectrum 400 spectrometer (Perkin Elmer). The spectra were obtained in transmittance mode in the region of 4000 cm^{-1} to 650 cm^{-1}, 16 scans and resolution of 4 cm^{-1}.

2.6. Scanning electron microscopy (SEM)

Morphological analyses were carried out using a MIRA 3 scanning electron microscope (Tescan), with FEG filament and secondary electron detector. The polymer film samples were previously metallized by depositing a 20 nm layer of gold-palladium using an SC7620 metallizer (Quorum Technologies).

2.7. X-ray Energy Dispersive Spectroscopy (EDS)

In order to clarify the morphology of the polymeric blends produced, qualitative chemical analysis was carried out by EDS to estimate the elemental spatial distribution of nitrogen (N) on the surface of the samples, so that this element is only present in the molecular structure of PNVCL. An X-ray analyzer accessory coupled to the SEM with the specifications of item 2.6 was used.

2.8. Fourier transform infrared spectromicroscopy (micro-FTIR)

FTIR measurements and chemical imaging were obtained to elucidate the composition of the different phases formed in the blends produced. The analyses were carried out at the Brazilian Synchrotron Light Laboratory (LNLS), at the National Center for Research in Energy and Materials (CNPEN). The FTIR spectra were collected in reflectance mode in the 4000 to 600 cm^{-1} region, with a spectral resolution of 4 cm^{-1} and 32 scans, using a Cary 670 spectrometer (Agilent). The FTIR microscopic image was obtained on a Cary 620 FTIR microscope (Agilent) combined with the spectrometer, equipped with liquid nitrogen-cooled elements and a focal plane array (FPA) detector with 4.096 elements and an optical configuration using 15 x objective lenses.

In order to meet the specification of a sample thickness of less than 5 μm for reflectance micro-FTIR analysis, sample preparation consisted of depositing a microdrop of the polymer blend solutions (following the procedure in item 2.4) on a gold (Au) substrate, which was then dried at room temperature for 18 hours.

2.9. Differential scanning calorimetry (DSC)

The thermal properties were investigated through DSC in a calorimeter Q2000 (TA Instrument). Each sample was submitted to cycles of heating, cooling and heating from -70 °C to 215 °C, at a rate of 10 °C.min^{-1}, under a nitrogen atmosphere, with flow rate of 50 mL.min^{-1}. In order to eliminate the thermal history resulting from processing and evaporation of the adsorbed moisture, the results of the second heating were considered for analysis. In this way, the crystallinity of the compounds induced in DSC was evaluated according to Equation 1[37]. Where ΔH_m and ΔH_c represent the melt enthalpy and crystallization enthalpy, respectively, obtained from the second heating curve of the samples; ΔH^0_m is the enthalpy of fusion of 100% crystalline PLA of 93.7 J.g^{-1} [36,38] and $\varnothing_m$ is the mass fraction of the semi-crystalline polymer.

$$Xc(\%) = \frac{\Delta H_m - \Delta H_c}{\Delta H_m^0 \times \varnothing_m} \times 100 \quad (1)$$

2.10. Thermogravimetric analysis (TGA)

The thermal stability of the samples was evaluated in the TGA 2 Stare System equipment (Mettler Toledo). The scans were performed in the temperature range between 30 and 600 °C, with a heating rate of 10 °C.min^{-1} and nitrogen atmosphere with flow rate of 50 mL.min^{-1}.

2.11. Contact angle measurements

The thermoresponsiveness of films were evaluated by measuring the contact angle of a microdrop (10 μL) of distilled water on the surfaces of the obtained films after 10 seconds of microdrop deposition. Contact angle measurements were performed using an Attension Theta optical tensiometer (Biolin Scientific), associated with the OneAttention software. The contact angle was determined through the arithmetic mean of the values obtained in three different regions of the surface of the samples at two different temperatures monitored by an infrared thermometer: at 25 ºC, below the phase transition temperature of the PNVCL, and at 50 ºC, above the transition temperature of the polymer.

2.12. Opacification test

This characterization was also performed to evaluate the thermoresponsiveness of the films. It consisted of observing the change in film opacity when moving 2 x 2 cm film samples from cold water to water heated at different temperatures, from 25 ºC to 45 ºC.

3. Results and discussion

3.1. Visual aspect

Figure 1 shows the images of the PLA, PNVCL and PNVCL/PLA 60/40 blend films obtained by solvent casting. Analyzing the macroscopic aspects of the samples, it can be seen that the PNVCL film is optically transparent, as expected because it is an amorphous polymer[38]. In contrast, the PLA film is translucent, indicating the presence of a semi-crystalline structure. Macroscopically, the films of the polymer blends had a heterogeneous appearance, with regions of the films that were translucent and others that were transparent.

3.2. Attenuated total reflectance Fourier transform infrared spectroscopy (ATR-FTIR)

Figure 2 shows schemes of PLA and PNVCL molecules. Their characteristic chemical groups were identified in the ATR-FTIR analysis, as shown in Figure 3 and Table 2.

The characteristic peaks of PNVCL were observed at 2926 cm^{-1} and 2855 cm^{-1}, associated with the symmetrical and asymmetrical vibrations of the C-H bond; at 1609 cm^{-1} referring to the C=O bond of the amide; at 1480 cm^{-1} related to the stretching of the C-N bond. The absence of the characteristic peaks of the monomer (vinyl group at 3108 cm^{-1}, 1656 cm^{-1} and 987 cm^{-1}) shows the success of the polymerization and purification procedures. The broad band in the region of 3400 cm^{-1} refers to the stretching of the O-H group, due to the highly hygroscopic nature of PNVCL and the formation of hydrogen bonds with the adsorbed moisture[3,11,39-41].

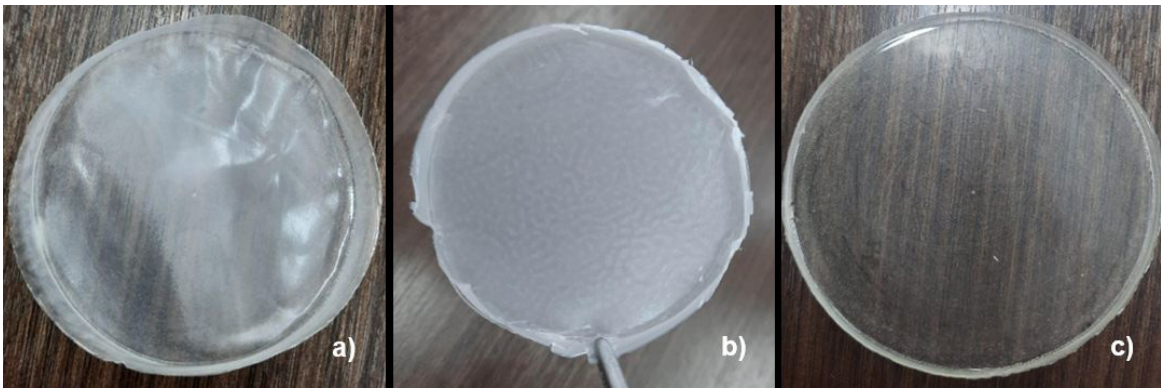

Figure 1. Films obtained by solvent casting of (a) PLA, (b) PNVCL/PLA 60/40 and (c) PNVCL.

The main peaks attributed to the functional groups of PLA appeared at 1748 cm^{-1} corresponding to the C=O carbonyl; at 1081 and 754 cm^{-1} referring to the stretching and deformation of the C–O from the esther group, respectively, and at 1453 cm^{-1} related to the stretching of the C–H methyl groups[42,43].

When analyzing the FTIR-ATR spectra of the PNVCL/PLA 40/60, 50/50 and 60/40 polymer blends, it was possible to notice the presence of some characteristic peaks of the precursor polymers, such as the symmetrical and asymmetrical vibrations of the PNVCL C–H bond, the C=O bond of the PNVCL amide, as well as the PLA amide, the stretching of the PNVCL C–N bond, the stretching of the C–H methyl groups, and stretching and deformations of the C–O from esther group, both from PLA, as described in Table 2. It is worth noting that in this analysis it was not possible to verify the shifting of the characteristic peaks of each polymer, which could indicate interaction between them, as reported in the studies by[7,44].

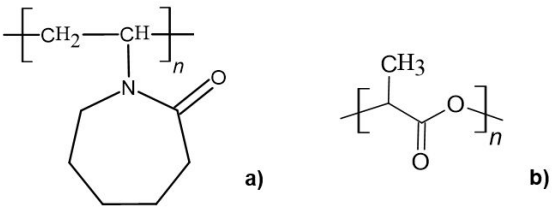

Figure 2. Molecular structure of a) PNVCL and b) PLA.

3.3. Scanning electron microscopy (SEM)

Figure 4 shows the SEM images of the blends' surfaces. It was possible to observe a heterogeneous morphology, with the presence of a continuous phase and another phase with spherical domains.

The increase of PNVCL concentration in the blends led to an increment in the size of the spherical domains, ranging from 13.7 ± 1.8 µm in the PNVCL/PLA 40/60 blend to 21.0 ± 2.4 µm in the PNVCL/PLA 60/40. This may be due to coalescence during the

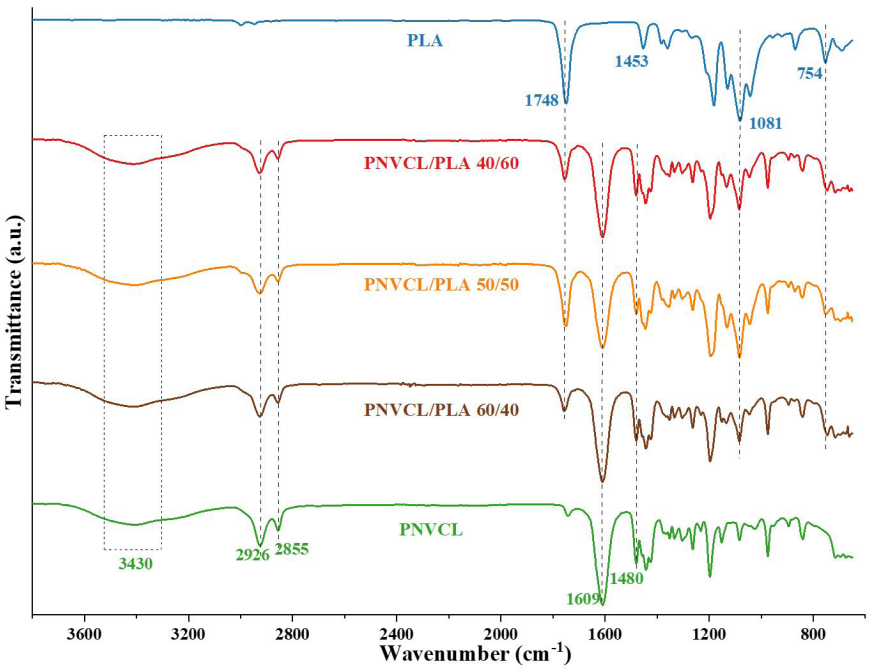

Figure 3. FTIR-ATR spectra of PLA, PNVCL and their blends.

Table 2. FTIR-ATR bands for PLA, PNVCL and their polymers blends.

Functional group	Wavenumber (cm^{-1})				
	PLA	PNVCL/PLA 40/60	PNVCL/PLA 50/50	PNVCL/PLA 60/40	PNVCL
Aliphatic C–H	-	2926; 2855	2926; 2855	2926; 2855	2926; 2855
C=O (ester)	1748	1754	1748	1754	-
C=O (amide)	-	1609	1609	1609	1609
C–N	-	1482	1480	1480	1480
C–H	1453	-	-	-	-
C–O–C	1081;754	1084; 748	1081; 750	1084; 745	-
O–H	-	3430	3430	3430	3430

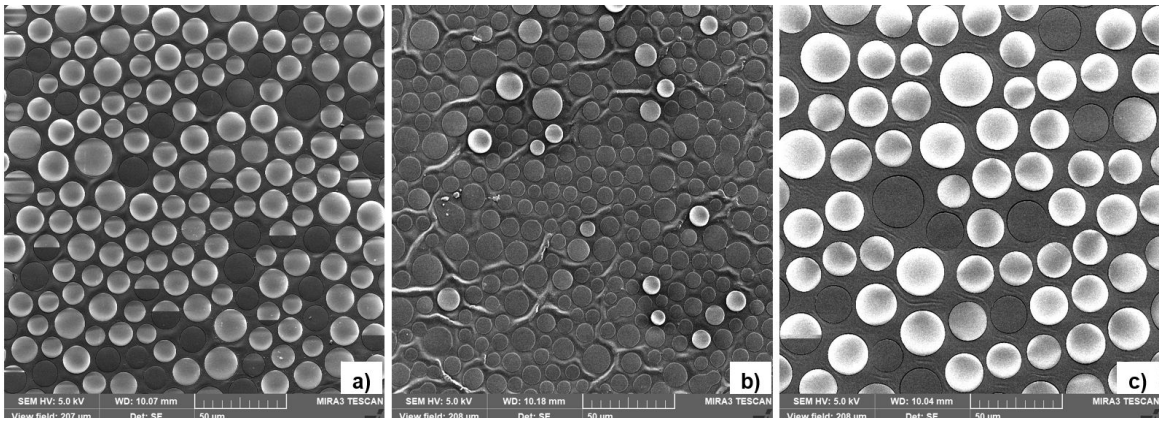

Figure 4. SEM imagens of polymer blends a) PNVCL/PLA 40/60 b) PNVCL/PLA 50/50 and c) PNVCL/PLA 60/40.

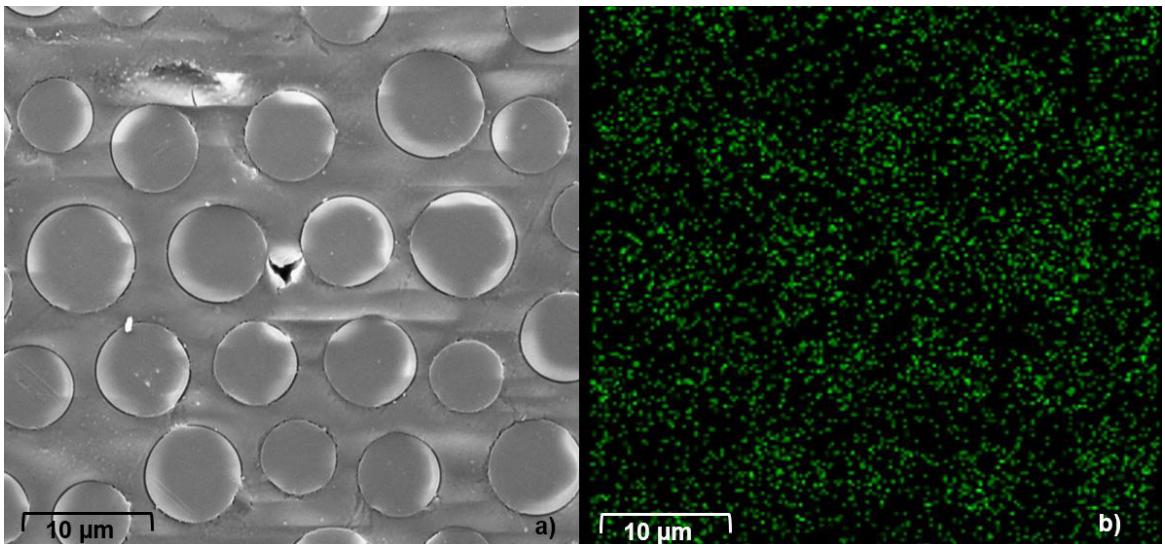

Figure 5. a) EDS image and b) EDS elemental mapping of nitrogen of the PNVCL/PLA 50/50 blend.

drying process from solvent casting. Coalescence depends on the concentration and viscosity of the components, as well as the types of interactions (hydrogen bonds, capillary forces, among others)[17].

In order to identify the polymers present in each of the phases, X-ray Energy Dispersive Spectroscopy (EDS) was performed.

3.4. X-ray Energy Dispersive Spectroscopy (EDS)

The results of the qualitative EDS chemical analysis show the spatial distribution of the nitrogen atoms (N) on the surface of the polymer blends, which can contribute to understanding the morphology of the blends produced, since the N atoms are only present in the PNVCL polymer. The EDS images were similar for the blends studied, as shown in Figure 5 (EDS images of the PNVCL/PLA 50/50 blend, as an example). Figure 5a shows the EDS image and Figure 5b shows the EDS mapping for the N element, indicated by the green color (the strong brightness represents greater elemental intensity). The images reveal that the N elements tend to be more concentrated in the region of the dispersed phase domains, although it is also possible to notice a certain distribution of this element in the matrix phase. Therefore, this result indicates the predominance of PNVCL in the dispersed phase, not excluding its presence in the continuous phase. Aiming to clarify and deepen this finding, an infrared analysis on a microscopic scale (micro-FTIR) was carried out.

3.5. Fourier Transform Infrared Spectromicroscopy (micro-FTIR)

Figure 6 shows the micro-FTIR spectra, magnified in the region between 1850 and 1550 cm^{-1}, corresponding to the spectral average of an area (400 x 400 µm) analyzed in each polymer blend. The peaks around 1766 cm^{-1} and 1629 cm^{-1} refer to the C=O bond of PLA and PNVCL, respectively. It is possible to see a variation in the absorbance intensity of these peaks in the different blends. For the PNVCL/PLA 40/60 blend, the peak referring to PLA at 1766 cm^{-1} shows the highest absorbance, proving its higher concentration in this sample. The PNVCL/PLA 50/50 blend has a similar absorbance intensity between the peaks analyzed. While the peak at 1629 cm^{-1}

referring to PNVCL appears more intense in the PNVCL/PLA 60/40 blend, due to the higher PNVCL contente in this blend.

The micro-FTIR results of all blends were similar, and the results for the PNVCL/PLA 60/40 blend are shown representatively in Figure 7. Figure 7a shows the microscopic image of a 200 µm x 200 µm cut-out of the area where the spectral average of the PNVCL/PLA 60/40 blend was obtained. By selecting the representative peaks of each polymer, at 1766 cm^{-1} for PLA and at 1629 cm^{-1} for PNVCL, the chemical absorbance maps were obtained in the form of a colored contour map (Figure 7b and 7c, respectively) for the selected area of the PNVCL/PLA 60/40 blend. For the absorbance maps, red indicates the maximum absorbance and blue the minimum absorbance.

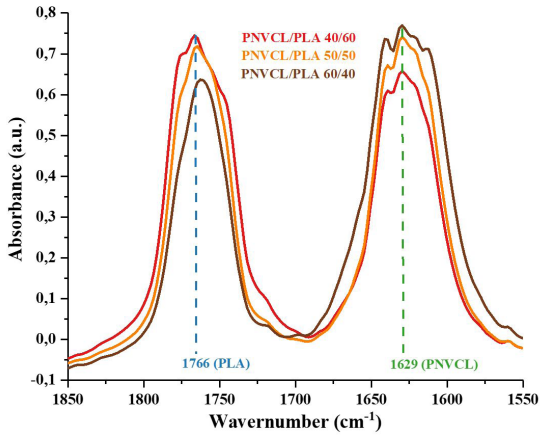

Figure 6. Micro-FTIR of the studied blends.

Thus, the absorbance map showed that PLA is predominantly present in the matrix phase of the blends, as observed by the red color, although its presence is also noted in the dispersed phase region. PNVCL shows maximum absorbance in the region of the domain phase, although its presence in the matrix phase can be seen in lower concentrations (lower intensity of color), in accordance with what was observed in the EDS analyses.

The coexistence of both polymers in varying concentrations in the different phases indicates the partial miscibility of the mixtures, which may be due to dipole-dipole intermolecular interactions between the carbonyl groups (C=O) present in the macromolecules, as was found in the study of Lu et al.[45] for the mixture of PLA and polycaprolactone (PCL).

3.6. Differential scanning calorimetry (DSC)

Figure 8 and Table 3 show the DSC results and data obtained for PLA, PNVCL and their polymer blends. The PLA film shows thermal transitions characteristic of a semi-crystalline structure[46] with a glass transition (T_g) at 61.6ºC, a cold crystallization temperature (T_{cc}) at 110.9ºC, as well as two melting temperatures (T_m) at 147.3ºC and 154.5ºC, resulting in 2.3% crystallinity. These values are intermediate to those reported in previous works[36,47-49]. The discrepancies found may be related to chemical composition and molar mass[50].

The appearance of the double endothermic melting peak of PLA in DSC second heating indicates the formation of heterogeneous crystalline structures during recrystallization within the DSC[51,52].

PNVCL is an amorphous polymer, and presented a T_g of 180.7 ºC. The difference between this value and other found in the literature[53,54], can be attributed mainly to polymer molar mass and its distribution.

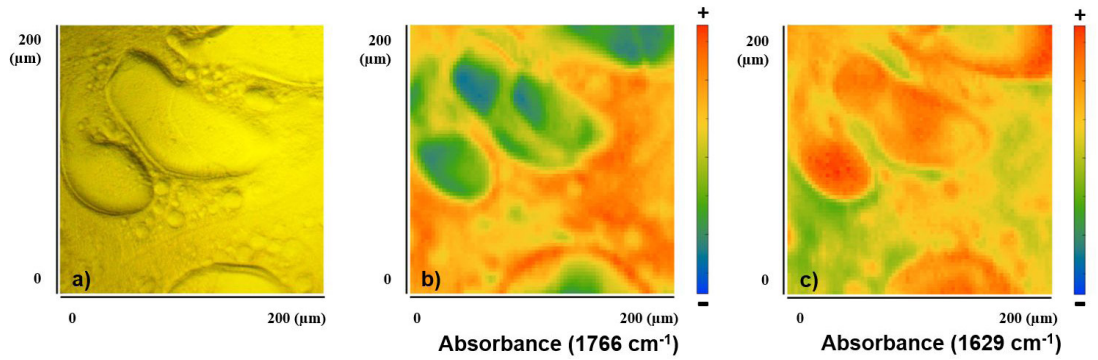

Figure 7. a) Optical microscopy image, b) absorbance chemical map at 1766 cm^{-1} and c) absorbance chemical map at 1629 cm^{-1} for the PNVCL/PLA 60/40 blend.

Table 3. Thermal Properties of the PLA, PNVCL and their polymer blends.

Sample	T_g (ºC) PLA	T_g (ºC) PNVCL	T_{cc} (ºC)	T_m (ºC)	X_c (%)
PNVCL	-	180.7	-	-	-
PLA	58.9	-	110.9	147.4 e 154.3	2.3
PNVCL/PLA 40/60	62.1	177.6	-	156.1	>1
PNVCL/PLA 50/50	62.0	176.7	-	153.7	>1
PNVCL/PLA 60/40	59.1	180.4	-	154.9	>1

In relation to the PNVCL/PLA polymer blends, it can be seen that they presented two glass transition temperatures, with values similar to those of the precursor materials, close to 62.0 ºC for the PLA phase and around 178.0 ºC for the PNVCL composition, confirming the biphasic character of the mixture[55]. In addition, it can be inferred that PLA crystallization is hindered in the blends, since T_{cf} is not evident, and T_m appears discreetly at around 154.0 ºC, for a degree of crystallinity of less than 1%. Therefore, for the thermal conditions applied, the presence of PNVCL in the blends acted as an impurity, preventing the PLA from crystallizing, similar to what was observed by previous authors[55] for the polyethylene terephthalate (PET) and polystyrene (PS) blends.

3.7. Thermogravimetric analysis (TGA)

The thermal stabilities of the materials were evaluated by thermogravimetry, according to the TGA curves and their derivatives (DTG curves) presented in Figure 9. The PLA film presented only one degradation step with mass loss of 98%, starting at 290 ºC, and a maximum mass loss rate at 368 ºC, similar to what was found in previous studies[56]. In turn, the PNVCL film exhibited a mass loss of 4% at around 98 ºC due to moisture elimination. The main stage of degradation of PNVCL is attributed to depolymerization[41], whith 90% of mass loss, na onset degradation temperature of 369 ºC and a temperature of maximum mass loss rateat 440 ºC.

PNVCL/PLA polymer blends presented three steps of mass loss that are associated with the events seen in pure polymers, namely: moisture loss, PLA degradation and PNVCL depolymerization. Moisture removal occurred before 200 ºC, with a mass loss of up to 20% for the PNVCL/PLA 50/50 blend. The PLA degradation step in the blends shifted to lower temperatures compared to pure PLA, with a maximum mass loss rate around 353 ºC, as can be seen in the DTG curves. The degradation temperature of PNVCL in the blends was similar to that observed in pure PNVCL film.

It was not possible to observe a correspondence in the mass losses of the polymers according to the proportions used to prepare the polymer blends. This can be explained by the heterogeneity of the blends and the small mass used for TGA analyses (less than 10 mg).

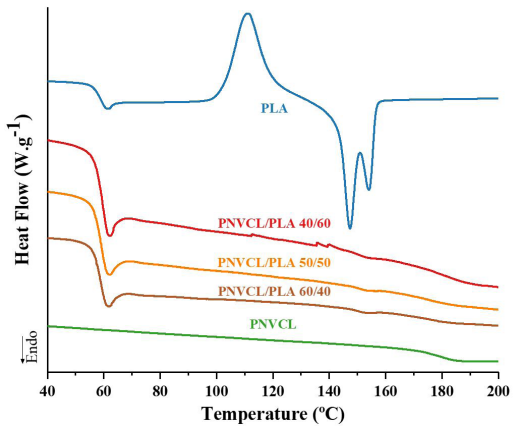

Figure 8. DSC results of PLA, PNVCL and their polymer blends.

3.8. Contact angle measurements

Figure 10 shows the images of the contact angle measurements of a water droplet on the surface of PLA, PNVCL, and PNVCL/PLA blends, analyzed at temperatures of 25 °C and 50 °C.

The absence of thermo-responsive properties is evident for the PLA film, as no variation in the contact angle is observed with temperature change. In contrast, the PNVCL film shows a significant variation in the contact angle, changing from 45.4 ° ± 2.1 ° to 80.0 ° ± 2.5 ° with increasing temperature. At 25 °C, the water droplet tends to spread more easily on the polymer surface due to its more hydrophilic state. On the other hand, at 50 °C, above the T_{PS}, there is a preference for polymer-polymer interaction, leading to a decrease in hydrophilicity.

The results of the blends also indicated thermo-responsive behavior, with a variation in the contact angle observed at the analyzed temperatures. Additionally, the increase of PNVCL content in the blends resulted in increased hydrophilicity of

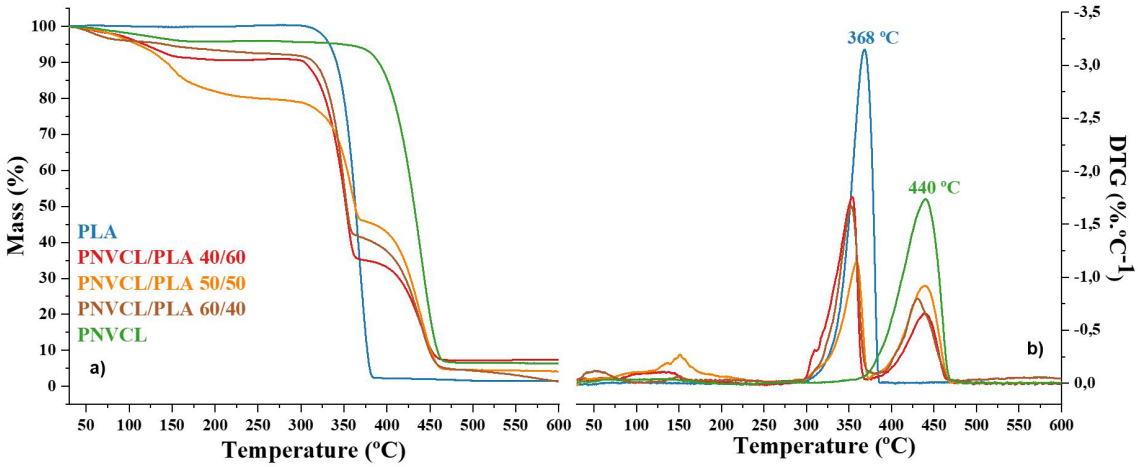

Figure 9. a) TGA and b) DTG curves of PLA, PNVCL and their polymer blends.

the mixtures, as evidenced by the reduction of contact angles under conditions below the T_{PS}, at 25 °C.

3.9. Opacification test

Figure 11 displays the images from the opacification test of the polymer films. The cloud point temperature (related to T_{PS}) of pure PNVCL in distilled water (concentration of 10% w.v^{-1}) is 32 ºC, as reported already in a previous work of our research group performed using the same PNVCL[7].

The analyses of blends indicated that the PNVCL/PLA 40/60, 50/50, and 60/40 blends began to exhibit opacification at 34 °C, 33 °C, and 32 °C, respectively. The reversibility of the turbidity of the solid films upon cooling could be observed almost instantaneously.

These results demonstrate a decrease in the cloud point temperature of the films with the increase of PNVCL content, indicating that the concentration of PNVCL in the samples is the predominant factor governing the thermorresponsive behavior of the films, as expected.

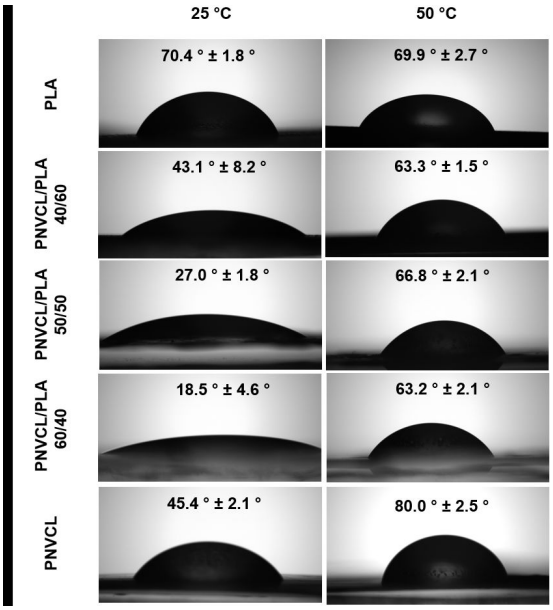

Figure 10. Images of contact angle measurements of PNVCL/PLA blend films and their precursor polymers at 25 and 50 ºC.

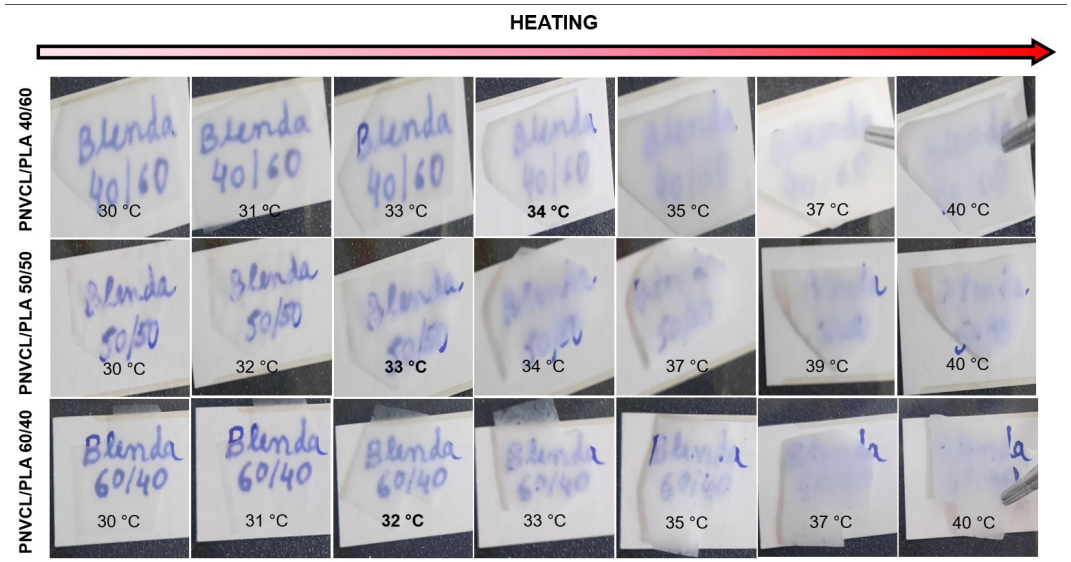

Figure 11. Images of the opacification analysis of solid blend films of PNVCL/PLA 40/60, 50/50, and 60/40.

4. Conclusions

Smart polymer blends of PNVCL/PLA were produced using the solvent casting method, with PNVCL weight contents of 40%, 50%, and 60%. The physicochemical and morphological characterizations demonstrated that the formed blends presented heterogeneous morphology. Through micro-FTIR analysis, it was possible to identify the distribution of the polymers in the phases observed in SEM, showing a prevalence of PNVCL in the dispersed phase and of PLA in the matrix phase. The polymer films from the blends exhibited thermo-responsiveness, as confirmed by the variation in contact angle and films opacity with temperature, with opacification temperatures observed between 34 °C and 32 °C, decreasing with the increase of PNVCL in the blends. Therefore, the physical mixing of PNVCL with PLA contributes to the improvement of properties of smart polymer systems, enabling new potential applications in the biomedical field, such as controlled drug release and smart dressings.

5. Acknowledgments

This work was financially supported by the National Council for Scientific and Technological Development (CNPq - Brazil) through the ongoing doctoral scholarship of G. R. C (Grant number 1401552/2022-9), as well as for A. N. G. G. scientific initiation scholarship (ID 220318946) through the Institutional Program for Scientific Initiation Scholarships (PIBIC/CNPq). D. A. O. and R. L. M. F. received master's scholarships from the Coordination for the Improvement of Higher Education Personnel (CAPES-Brazil).

The authors would like to thank the Petrochemistry Laboratory (LPQ), Fuels Laboratory (LAC), and Composite Materials and Structural Integrity Laboratory (CompoLab) of Petroleum and Energy Research Institute (i-LITPEG), as well as the Polymer Laboratory (LabPol) and Electron Microscopy Laboratory (LME) of National Institute of Union Technology and Coating of Materials (INTM) of Federal University of Pernambuco (UFPE).

This research used facilities of the Brazilian Synchrotron Light Laboratory (LNLS), part of the Brazilian Center for Research in Energy and Materials (CNPEM), a private non-profit organization under the supervision of the Brazilian Ministry for Science, Technology, and Innovations (MCTI). The IMBUIA-Micro beamline staff is acknowledged for the assistance during the experiments (proposal number 20232963).

6. References

1. Zhang Q, Weber C, Schubert US, Hoogenboom R. Thermoresponsive polymers with lower critical solution temperature: from fundamental aspects and measuring techniques to recommended turbidimetry conditions. Mater Horiz. 2017;4(2):109-16. http://doi.org/10.1039/C7MH00016B.
2. Gandhi A, Paul A, Sen SO, Sen KK. Studies on thermoresponsive polymers: phase behaviour, drug delivery and biomedical applications. Asian J Pharm Sci. 2015;10(2):99-107. http://doi.org/10.1016/j.ajps.2014.08.010.
3. Cerqueira GR, Feitosa RLM, Henrique MA, Andrade MF, Trindade FCS, Araujo ES, et al. Grafting of poly(*N*-vinylcaprolactam) in polyurethane by gamma radiation. Radiat Phys Chem. 2024;217:111476. http://doi.org/10.1016/j.radphyschem.2023.111476.
4. Saha P, Kather M, Banerjee SL, Singha NK, Pich A. Aqueous solution behavior of thermoresponsive polyzwitterionic microgels based on poly(N-vinylcaprolactam) synthesized via RAFT precipitation polymerization. Eur Polym J. 2019;118:195-204. http://doi.org/10.1016/j.eurpolymj.2019.05.063.
5. Winninger J, Iurea DM, Atanase LI, Salhi S, Delaite C, Riess G. Micellization of novel biocompatible thermo-sensitive graft copolymers based on poly(ε-caprolactone), poly(N-vinylcaprolactam) and poly(N-vinylpyrrolidone). Eur Polym J. 2019;119:74-82. http://doi.org/10.1016/j.eurpolymj.2019.07.015.
6. Nieuwenhove IV, Maji S, Dash M, Vlierberghe SV, Hoogenboom R, Dubruel P. RAFT/MADIX polymerization of N-vinylcaprolactam in waterethanol solvent mixtures. Polym Chem. 2017;8(16):2433-7. http://doi.org/10.1039/C6PY02224C.
7. Oliveira DA, Cerqueira GR, Feitosa RLM, Marini J, Almeida YMB, Morelli CL. Thermoresponsive blends formed by poly(*N*-vinylcaprolactam) and thermoplastic polyurethane. J Appl Polym Sci. 2024;141(43):e56123. http://doi.org/10.1002/app.56123.
8. Rosa VR, Woisel P, Hoogenboom R. Supramolecular control over thermoresponsive polymers. Mater Today. 2016;19(1):44-55. http://doi.org/10.1016/j.mattod.2015.06.013.
9. Cortez-Lemus NA, Licea-Claverie A. Poly(*N*-vinylcaprolactam), a comprehensive review on a thermoresponsive polymer becoming popular. Prog Polym Sci. 2016;53:1-51. http://doi.org/10.1016/j.progpolymsci.2015.08.001.
10. Gholiha HM, Ehsani M, Saeidi A, Ghadami A, Alizadeh N. Magnetic dual-responsive semi-IPN nanogels based on chitosan/PNVCL and study on BSA release behavior. Prog Biomater. 2021;10(3):173-83. http://doi.org/10.1007/s40204-021-00161-8. PMid:34370266.
11. Flores-Rojas GG, López-Saucedo F, Vázquez E, Hernández-Mecinas E, Huerta L, Cedillo G, et al. Synthesis of polyamide-6@cellulose microfilms grafted with N-vinylcaprolactam using gamma-rays and loading of antimicrobial drugs. Cellulose. 2020;27(5):2785-801. http://doi.org/10.1007/s10570-020-02986-1.
12. González-Hernández G, Pino-Ramos VH, Islas L, Alvarez-Lorenzo C, Concheiro A, Bucio E. Radiation-grafting of N-vinylcaprolactam and 2-hydroxyethyl methacrylate onto polypropylene films to obtain a thermo-responsive drug delivery system. Radiat Phys Chem. 2019;157:6-14. http://doi.org/10.1016/j.radphyschem.2018.12.014.
13. Pino-Ramos VH, Flores-Rojas GG, Alvarez-Lorenzo C, Concheiro A, Bucio E. Graft copolymerization by ionization radiation, characterization, and enzymatic activity of temperature-responsive SR-g -PNVCL loaded with lysozyme. React Funct Polym. 2018;126:74-82. http://doi.org/10.1016/j.reactfunctpolym.2018.03.002.
14. Doberenz F, Zeng K, Willems C, Zhang K, Groth T. Thermoresponsive polymers and their biomedical application in tissue engineering – a review. J Mater Chem B Mater Biol Med. 2020;8(4):607-28. http://doi.org/10.1039/C9TB02052G. PMid:31939978.
15. Sala RL, Kwon MY, Kim M, Gullbrand SE, Henning EA, Mauck RL, et al. Thermosensitive poly(*N*-vinylcaprolactam) injectable hydrogels for cartilagem tissue engineering. Tissue Eng Part A. 2017;23(17-18):935-45. http://doi.org/10.1089/ten.tea.2016.0464. PMid:28384053.
16. Rao KM, Rao KS, Ha C. Stimuli responsive poly(vinyl caprolactam) gels for biomedical applications. Gels. 2016;2(1):6. http://doi.org/10.3390/gels2010006. PMid:30674138.
17. Ajitha AR, Thomas S. Compatibilization of polymer blends. Cham: Elsevier; 2020. p. 1-29. http://doi.org/10.1016/B978-0-12-816006-0.00001-3.
18. Silva DF, Luna CBB, Araújo EM, Silva AL. Blendas poliméricas: conceitos, obtenção e aplicações. Rev Eng Tecnol. 2016 [cited

2024 Jan 23]. 8(1):58-77. Available from: https://revistas.uepg.br/index.php/ret/article/view/11663.

19. Utracki LA, Mukhopadhyay P, Gupta RK. Polymer blends: introduction. In: Utracki LA, Wilkie CA, editors. Polymer blends handbook. Cham: Springer Science; 2014. p. 3-170. http://doi.org/10.1007/978-94-007-6064-6.
20. Guo Y, Li N, Chen X, Wang T, Zhang W, Wu L. Fabrication of biocompatible transdermal nanofibrous patch for localized delivery of lidocaine and Rosemary oil to improve effective management of lymphoma pain and nursing care. Indian J Pharm Educ Res. 2024;58(3):771-83. http://doi.org/10.5530/ijper.58.3.85.
21. Samiullah K, Abdur R, Faisal BS, Gamal S, Amira M, Fakhreldeen D. Fabrication and in vitro evaluation of pH/termo dual responsive hydrogels as controlled ibuprofen sodium in situ depot. Des Monomers Polym. 2025;28(1):1-15. http://doi.org/10.1080/15685551.2024.2442118.
22. Espinosa-Dsib A, Chen J, Zavgorodnya O, Kozlovskaya V, Liang X, Kharlampieva E. Tuning assemby and enzymatic degradation of silk/poly(N-vinylcaprolactam) multilayers via molecular weight and hydrophobicity. Soft Matter. 2015;11(25):5133-45. http://doi.org/10.1039/C5SM00464K. PMid:26041120.
23. Nahra SR, Oliveira MP, Macedo EF, Hurtado CR, Tada DB, Guerrini LM, et al. Development of scaffolds based in blends of poly(N-vinylcaprolactam) and poly(N-vinylcaprolactam-co-butylacrylate) with poly(3-hexylthiophene) for tissue engineering: synthesis, processing, characterization, and biological assay. J Appl Polym Sci. 2022;139(41):e53006. http://doi.org/10.1002/app.53006.
24. Sta M, Aguiar G, Forni AAJ, Medeiros SF, Santos AM, Demarquette NR. Design and characterization of PNVCL-based nanofibers and evaluation of their potential applications as scaffolds for surface drug delivery of hydrophobic drugs. J Appl Polym Sci. 2020;137(11):48472. http://doi.org/10.1002/app.48472.
25. Li H, Liu K, Williams GR, Wu J, Wang H, Niu S, et al. Dual temperature and pH responsive nanofiber formulations prepared by electrospinning. Colloids Surf B Biointerfaces. 2018;171:142-9. http://doi.org/10.1016/j.colsurfb.2018.07.020. PMid:30025376.
26. Schneider F, Balaceanu A, Di Z, Melnichenko YB, Allgaier J, Pich A, et al. Internal structure and phase transition behavior of stimuli-responsive microgels in PEG melts. Soft Matter. 2017;13(15):2738-48. http://doi.org/10.1039/C6SM02501C. PMid:28217774.
27. Feldstein MM, Bovaldinova KA, Bermesheva EV, Moscalets AP, Dormidontova EE, Grinberg VY, et al. Thermo-switchable pressure-sensitive adhesives based on poly(N-vinyl caprolactam) non-covalently cross-linked by poly(ethylene glycol). Macromolecules. 2014;47(16):5759-67. http://doi.org/10.1021/ma501191k.
28. Petrov MM, Makhaeva EE, Keshtov ML, Khokhlov AR. The effect of poly(*N*-vinylcaprolactam) on t2he electrochromic properties of a poly(pyridinium triflate). Electrochim Acta. 2014;122:159-65. http://doi.org/10.1016/j.electacta.2013.09.013.
29. Sinha MK, Purkait MK. Preparation and characterization of stimuli-responsive hydrophilic polysulfone membrane modified with poly (N-vinylcaprolactam-co-acrylic acid). Desalination. 2014;348:16-25. http://doi.org/10.1016/j.desal.2014.06.007.
30. Kalivoda A, Fischbach M, Kleinebudde P. Application of mixtures of polymeric carriers for dissolution enhancement of oxeglitazar using hot-melt extrusion. Int J Pharm. 2012;439(1-2):145-56. http://doi.org/10.1016/j.ijpharm.2012.10.013. PMid:23073606.
31. Kalivoda A, Fischbach M, Kleinebudde P. Application of mixtures of polymeric carriers for dissolution enhancement of fenofibrate using hot-melt extrusion. Int J Pharm. 2012;429(1-2):58-68. http://doi.org/10.1016/j.ijpharm.2012.03.009. PMid:22440149.
32. Paneysar JS, Barton S, Chandra S, Ambre P, Coutinho E. Novel thermoresponsive assemblies of co-grafted natural and synthetic polymers for water purification. Water Sci Technol. 2017;75(5-6):1084-97. http://doi.org/10.2166/wst.2016.599. PMid:28272038.
33. Jia H, Hou Y, Zhang M, Pan Y, Liu C, Shen C, et al. SC crystals of porous PLA via thermally–induced phase separation: effects of process conditions, solvent composition and nucleating agent. Eur Polym J. 2024;213:113095. http://doi.org/10.1016/j.eurpolymj.2024.113095.
34. Wang H, Wang L, Liu Z, Luo Y, Kang Z, Che X. Astragaloside/PVP/PLA nanofiber functional dressing prepared by coaxial electrostatic spinning technology for promoting diabetic wound healing. Eur Polym J. 2024;210:112950. http://doi.org/10.1016/j.eurpolymj.2024.112950.
35. Taib NAAB, Rahman MR, Huda D, Kuok KK, Hamdan S, Bakri MKB, et al. A review on poly lactic acid (PLA) as a biodegradable polymer. Polym Bull. 2023;80(2):1179-213. http://doi.org/10.1007/s00289-022-04160-y.
36. Shuhua W, Qiaoli X, Fen L, Jinming D, Husheng J, Bingshe X. Preparation and proprerties of celulose-based carbon microsphere/poly(lactic acid) composites. J Compos Mater. 2013;48(11):1297-302. http://doi.org/10.1177/0021998313485263.
37. Nguyen TL, Bédoui F, Mazeran PE, Guigon M. Mechanical investigation of confined amorphous phase in semicrystalline polymers: case of PET and PLA. Polym Eng Sci. 2015;55(2):397-405. http://doi.org/10.1002/pen.23896.
38. Meng B, Deng J, Liu Q, Wu Z, Yang W. Transperent and ductile poly(lactic acid)/poly(butyl acrylate) (PBA) blends: structure and proprieties. Eur Polym J. 2012;48(1):127-35. http://doi.org/10.1016/j.eurpolymj.2011.10.009.
39. Halligan E, Zhuo S, Colbert DM, Alsaadi M, Tie BSH, Bezerra GSN, et al. Modulation of the lower critical solution temperature of thermoresponsive poly(*n*-vinylcaprolactam) utilizing hydrophilic and hydrophobic monomers. Polymers (Basel). 2023;15(7):1595. http://doi.org/10.3390/polym15071595. PMid:37050207.
40. Cornejo-Bravo JM, Palomino K, Palomino-Vizcaino G, Pérez-Landeros OM, Curiel-Alvarez M, Valdez-Salas B, et al. Poly(*N*-vinylcaprolactam) and salicylic acid polymeric prodrug grafted onto medical silicone to obtain a novel thermo- and pH-responsive drug delivery system for potential medical devices. Materials (Basel). 2021;14(5):1065. http://doi.org/10.3390/ma14051065. PMid:33668741.
41. Kozanoglu S, Ozdemir T, Usanmaz A. Polymerization of N-vinylcaprolactam and characterization of poly(*N*-vinylcaprolactam). J Macromol Sci Part A Pure Appl Chem. 2011;48(6):467-77. http://doi.org/10.1080/10601325.2011.573350.
42. Grabowska B, Kaczmarska K, Cukrowicz S, Mączka E, Bobrowski A. Polylactide used as filment in 3D printing–part 1: FTIR, DRIFT and TG-DTG studies. J Cast Mater Eng. 2020;4(3):48-52. http://doi.org/10.7494/jcme.2020.4.3.48.
43. Paragkumar T, Edith D, Jean-Luc S. Surface characteristics of PLA and PLGA films. Appl Surf Sci. 2006;253(5):2758-64. http://doi.org/10.1016/j.apsusc.2006.05.047.
44. Sabahi N, Roohami I, Wang CH, Farajzadeh E, Li X. Thermoplastic polyurethane-based shape memory polymers with potential biomedical application: the effect of TPU soft-segment on shape memory effect and cytocompatibility. Polymer (Guildf). 2023;283:126189. http://doi.org/10.1016/j.polymer.2023.126189.
45. Lu H, Shinzawa H, Kazarian SG. Intermolecular interactions in the polymer blends under high-pressure CO2 studied using two-dimensional correlation analysis and two-dimensional disrelation mapping. Appl Spectrosc. 2021;75(3):250-8. http://doi.org/10.1177/0003702820978473. PMid:33231478.
46. Gao C, Bao X, Yu L, Liu H, Simon GP, Chen L, et al. Thermal properties and miscibility of semi-crystalline and amorphous PLA blends. J Appl Polym Sci. 2014;131(23):41205. http://doi.org/10.1002/app.41205.

47. Santana L, Alves JL, Netto ACS, Merlini C. Estudo comparativo entre PETG e PLA para impressão 3D através de caracterização térmica, química e mecânica. Rev Materia (Rio J). 2018;23(4):e12267. http://doi.org/10.1590/S1517-707620180004.0601.
48. Shuhua W, Qiaoli X, Fen L, Jinming D, Husheng J, Bingshe X. Preparation and proprerties of celulose-based carbon microsphere/poly(lactic acid) composites. J Compos Mater. 2014;48(11):1297-302. http://doi.org/10.1177/0021998313485263.
49. Cuiffo MA, Snyder J, Elliott AM, Romero N, Kannan S, Halada G. Impacto f the fused deposition (FDM) printing processo n polylactic acid (PLA) chemistry and structure. Appl Sci (Basel). 2017;7(6):579. http://doi.org/10.3390/app7060579.
50. Fang Q, Hanna MA. Rheological properties of amorphous and semicrystalline polylactic acid polymers. Ind Crops Prod. 1999;10(1):47-53. http://doi.org/10.1016/S0926-6690(99)00009-6.
51. Shazleen SS, Foong NLY, Ibrahim NA, Hassan MA, Ariffin H. Combined effects of cellulose nanofiber nucleation and maleated polylactic acid compatibilization on the crystallization kinetic and mechanical properties of polylactic acid nanocomposite. Polymers (Basel). 2021;13(19):3226. http://doi.org/10.3390/polym13193226. PMid:34641040.
52. Parida C, Dash S, Chaterjee P. The thermal and crystallization studies of luffa fiber reinforced poly lactic acid composites, open. J Compos Mater. 2016;6(1):1-7. http://doi.org/10.4236/ojcm.2016.61001.
53. Fallon M, Halligan S, Pezzoli R, Geever L, Higginbotham C. Synthesis and characterisation of novel temperature and pH sensitive physically cross-linked poly(N-vinylcaprolactam-co-itaconic acid) hydrogels for drug delivery. Gels. 2019;5(3):41. http://doi.org/10.3390/gels5030041. PMid:31470691.
54. Halligan SC, Dalton MB, Murray KA, Dong Y, Wang W, Lyons JG, et al. Synthesis, characterisation and phase transition behaviour of temperature-responsive physically crosslinked poly(*N*-vinylcaprolactam) based polymers for biomedical applications. Mater Sci Eng C. 2017;79:130-9. http://doi.org/10.1016/j.msec.2017.03.241. PMid:28628999.
55. Wellen RMR, Rabello MS. Redução da velocidade de cristalização a frio do PET na presença de poliestireno. Polímeros. 2007;17(2):113-22. https://doi.org/10.1590/S0104-14282007000200010.
56. Krishnaiah P, Ratnam CT, Manickam S. Development of silane grafted halloysite nanotube reinforced polylactide nanocomposites for the enhancement of mechanical, termal and dynamic-mechanical properties. Appl Clay Sci. 2017;135:583-95. http://doi.org/10.1016/j.clay.2016.10.046.

Data Availability

Data will be made available on request.